This article was downloaded by:
On: *26 January 2011*
Access details: *Access Details: Free Access*
Publisher *Taylor & Francis*
Informa Ltd Registered in England and Wales Registered Number: 1072954 Registered office: Mortimer House, 37-41 Mortimer Street, London W1T 3JH, UK

Liquid Crystals
Publication details, including instructions for authors and subscription information:
http://www.informaworld.com/smpp/title~content=t713926090

Direct observation of smectic layers in side chain liquid crystal polymer films

I. G. Voigt-martin[a]; H. Durst[b]
[a] Institut für Physikalische Chemie der Universität Mainz, Jakob-Welder Weg 15, Mainz, F.R. Germany
[b] Max-Planck-Institut für Polymerfoschung, Mainz, F.R. Germany

To cite this Article Voigt-martin, I. G. and Durst, H.(1987) 'Direct observation of smectic layers in side chain liquid crystal polymer films', Liquid Crystals, 2: 5, 601 — 610
To link to this Article: DOI: 10.1080/02678298708086318
URL: http://dx.doi.org/10.1080/02678298708086318

PLEASE SCROLL DOWN FOR ARTICLE

Full terms and conditions of use: http://www.informaworld.com/terms-and-conditions-of-access.pdf

This article may be used for research, teaching and private study purposes. Any substantial or systematic reproduction, re-distribution, re-selling, loan or sub-licensing, systematic supply or distribution in any form to anyone is expressly forbidden.

The publisher does not give any warranty express or implied or make any representation that the contents will be complete or accurate or up to date. The accuracy of any instructions, formulae and drug doses should be independently verified with primary sources. The publisher shall not be liable for any loss, actions, claims, proceedings, demand or costs or damages whatsoever or howsoever caused arising directly or indirectly in connection with or arising out of the use of this material.

Liquid Crystals, 1987, Vol. 2, No. 5, 601–610

Direct observation of smectic layers in side chain liquid crystal polymer films

by I. G. VOIGT-MARTIN
Institut für Physikalische Chemie der Universität Mainz, Jakob-Welder Weg 15, Mainz, F.R. Germany
and H. DURST
Max-Planck-Institut für Polymerfoschung, Mainz, F.R. Germany

(*Received 23 December 1986; accepted 9 May 1987*)

By applying stringent conditions to the imaging process it has been possible to produce electron micrographs of the smectic planes in a highly beam sensitive polymethcrylate side chain liquid crystal polymer. These planes show a high degree of internal perfection, while, at the same time, showing clear evidence of curvature. The director orientation was determined over a fairly large region.

Downloaded At: 16:29 26 January 2011

1. Introduction

The production and interpretation of lattice images, particularly from beam sensitive samples, is by no means a trivial matter. However, the purpose of stressing the problems involved is not that of self-congratulation. Rather, it is the only means of proving that it has been possible to obtain images of what we claim to be seeing, namely the smectic planes in a side chain liquid crystal polymer. It is essential to state the experimental conditions under which the images were obtained in order to ensure that we are operating under phase contrast conditions. Furthermore image interpretation is only possible after making the appropriate calculations in order to decide whether dynamical or kinematical scattering theory has to be applied. Those who are informed about the theory of image formation in the electron microscope will, quite rightly, refuse to interpret an image unless these conditions are clearly stated.

2. Sample preparation

Thin films of the side chain liquid crystal polymer described in the preceding paper (1987, *Liquid Crystals*, **2**, 585, and hereafter denoted by I) were prepared either by spin coating or by spreading a drop of the polymer in solution on to water. In both cases there is some pre-alignment, which, however, does not produce small angle diffraction maxima in the diffraction pattern. Only after annealing in the smectic phase just below the smectic–nematic transition is orientation achieved, as evidenced by the appearance of three orders of a small angle electron diffraction peak corresponding to a spacing of 28·48 Å. The texture of the films under the light microscope indicates the appearance of rather large batônnets, which eventually form a focal conic structure.

3. High resolution electron microscopy

In order to obtain more detailed information about the smectic layers within the regions giving rise to smectic diffraction patterns (cf. I), it is necessary to turn to high

resolution electron microscopy. Although the layers which are to be resolved have a spacing of 28·48 Å which does not lie in the high resolution range for electron microscopy, nevertheless the microscope alignment must be performed with an extremely high degree of precision in order to be able to image the smectic planes in these extremely beam sensitive materials. The following problems are involved:

(*a*) destruction of the sample due to beam damage;
(*b*) specimen drift;
(*c*) correction for astigmatism;
(*d*) adjustment of the correct defocusing value;
(*e*) calculation of the extinction distance;
(*f*) image processing.

These points will now be discussed.

3.1. *Destruction of the sample due to beam damage*

It is well known that the electron beam causes both material loss and loss of diffraction contrast in biological and polymeric samples [1]. Destruction of the sample is easily recognized by characteristic changes in the diffraction patterns of crystalline (or liquid-crystalline) samples. The diffraction maxima become more diffuse and subsequently change spacing before disappearing altogether. Depending on the sample, this problem can be alleviated by the use of sub-visual intensities and low temperatures [2]. While this technique is adequate for low resolution, it cannot be applied for medium to high resolution because in this case high intensity is necessary for extremely fine astigmatism correction and correct adjustment of the defocusing value. Therefore the use of a low dose unit is mandatory. In this case the area of interest is first imaged at low magnification with negligible radiation. Subsequently the beam is shuttered above the specimen and the required magnification selected. Supplementary beam and image shift functions are now switched on, so that an area adjacent to the one of interest is displayed after removal of the shutter. The imaging conditions are optimized on this adjacent area. Subsequently the shift functions are switched off and the area of interest exposed.

Downloaded At: 16:29 26 January 2011

3.2. *Drift during exposure*

It is necessary to make a compromise during exposure of the sample area. The use of low intensities minimises specimen destruction but prolongs beam exposure, so that specimen drift will prevent high resolution imaging. Consequently the exposure time must be kept as short as possible and specimen damage reduced during exposure. The latter can be achieved by the use of a cryo-stage; however this must be capable of producing high resolution. Such resolution tests have been performed on the three cooling holders currently available for the Philips 420 electron microscope [3]: the original Philips cooling holder, type PW 6591, the new Philips cryo-holder type PW 6599 and an older version of the Gatan cooling holder. While there are some differences in detail between the holders, they are all capable, in principle, of producing high resolution images in the range required here. Details, such as good temperature control and convenient specimen exchange, led to a decision on our part in favour of the new Gatan cryo holder. In view of the increased specimen drift at low temperatures, it is advisable to use intermediate magnification rather than very high magnification and reduce the exposure time. Drift is further reduced by stabilizing the specimen on a carbon film.

3.3. *Astigmatism correction*

For high resolution work the requirements regarding astigmatism correction of the objective lens are very severe. In view of the necessity of using a carbon film to stabilize the sample, it was natural to use the optical transform of the supporting carbon film as a check for astigmatism [4]. When the Thon rings from the carbon films, as observed in the optical diffractometer, were truly circular thus indicating good astigmatism correction, and furthermore when the resolution had been tested by the extent of the Thon rings, [5] then the microscope was judged to have been adjusted correctly for high resolution work (cf. figure 1). The Thon rings are also a good test for specimen drift.

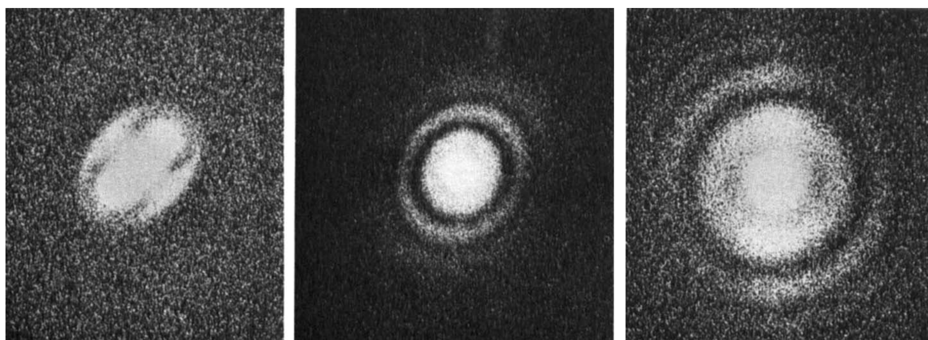

Figure 1. Correction for astimatism as judged by the optical transform of the carbon film.

Downloaded At: 16:29 26 January 2011

3.4. *Adjustment of the correct defocusing value*

Having achieved optimum alignment of the microscope, it is necessary to consider how contrast variations in the specimen, enabling us to image lattice planes, are to be achieved at all. The individual lattice planes are imaged by phase contrast. This is produced by the interference of the scattered electron wave that passes through the objective aperture with the unscattered, or background, electron wave, while amplitude contrast is produced by the loss of electrons which are scattered outside the objective aperture.

As we have discussed previously [6] the electron microscopic image is produced by a two stage process, involving first the production of a diffraction pattern (Fourier transform of the object function) and subsequently the production of an image (Fourier transform of the image function). It is convenient to express this mathematically [7]. The specimen can be described by a function $\sigma(x, y)$ giving the projected density in atoms per unit area at object plane coordinates x, y. The object transform is defined as

$$T^0(\alpha, \theta) = \iint \sigma(x, y) \exp i\left\{-\left(\frac{2\pi}{\lambda}\right)[x\alpha\cos\theta + y\alpha\sin\theta]\right\} dx\, dy,$$

where the transform is given circular coordinates α/λ and θ. α is the scattering angle, λ the electron wavelength and θ the azimuthal coordinate. In the wave theory of image formation, spherical aberration of the objective lens C_s and defocusing Δf lead to a phase shift $\chi(\alpha)$ which the scattered wave undergoes at the diffraction plane of the

microscope. The image transform is then given by

$$T^{i}_{\mathrm{tot}}(\alpha, \theta) = -T^{0}(\alpha, \theta) f(\alpha) A(\alpha)[\sin\chi(\alpha) + Q(\alpha)\cos\chi(\alpha)],$$

where $f(\alpha)$ is the atomic scattering factor and the objective aperture is accounted for by the aperture function $A(\alpha)$. The transform of the phase contrast image is related to the transform of the object by

$$T^{i}_{\mathrm{phase}}(\alpha, \theta) = -T^{0}(\alpha, \theta) A(\alpha) f(\alpha) \sin\chi(\alpha),$$

and the transform of the amplitude contrast image is related to the transform of the object by

$$T^{i}_{\mathrm{ampl}}(\alpha, \theta) = -T^{0}(\alpha, \theta) A(\alpha) f(\alpha) Q(\alpha) \cos\chi(\alpha),$$

where

$$\chi(\alpha) = \frac{2\pi}{\lambda}[-\tfrac{1}{4}C_s\alpha^4 + \tfrac{1}{2}\Delta f\alpha^2].$$

Therefore in order to produce the phase contrast required for imaging the smectic planes with a spacing of 28 Å it was necessary to calculate the phase contrast transfer function for the Philips EM 420 operated at 100 kV; this is shown in figure 2 for various defocus values. These results clearly show the physical significance of the phase retardation. When $\Delta f = 0$, $\chi(\alpha)$ is determined only by spherical aberration and is essentially zero except at high α/λ values which do not concern us here. Optimum defocusing for high resolution would appear to be achieved at $\Delta f = 1000$ Å, where $\sin\chi(\alpha)$ is close to unity over a large range of resolutions, but consideration of the α value involved in the imaging of 28 Å planes, which is in the small angle range, indicates that we require a higher defocusing value. However, the results in figure 2 show that these higher values introduce high frequency noise, as well as eventually leading to a lack of sharpness in the image. Therefore an aperture was introduced in the back focal plane which is large enough to transmit several diffracted beams for the imaging process but small enough to eliminate the high frequency noise.

Downloaded At: 16:29 26 January 2011

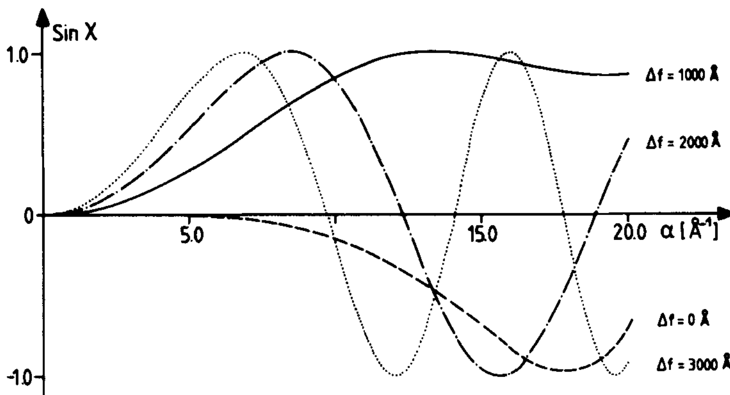

Figure 2. The phase contrast transfer function for the Philips EM 420 at 100 kV for different values of defocus; this was calculated with $C_s = 2$ mm and $\lambda = 0{\cdot}037$ Å.

3.5. *Image formation*

Areas giving rise to the smectic type diffraction pattern (cf. figure 3) were selected. Subsequently the electron microscope was adjusted on an adjacent area as described

Figure 3. Electron diffraction pattern obtained from the side chain liquid crystal polymer.

Downloaded At: 16:29 26 January 2011

previously before the area of interest was exposed to the electron beam. Figure 4 shows the images of the smectic layers. In order to compare these micrographs with the dark field data of figure 9 of I (n.b. the difference in magnification is 20 ×) we note that the regions in which lattice images are observed correspond in dimension to the bright domains which appeared in the dark field images. From the direction of the diffraction pattern it was deduced in I that the smectic layers are perpendicular to the long edges of the elongated regions. That this interpretation was correct is confirmed here. However, over and above the general information about their average direction and distribution of the smectic regions in the specimen, this micrograph demonstrates details of the structure within these regions, namely, the actual appearance of the individual smectic planes as well as information about their degree of perfection. Details are left for §4. Measurement of the distance between the observed planes confirms the distance of 28 Å.

3.6. *Calculation of the extinction distance*

The interpretation of lattice images appears simple, but a number of papers, following Menter's classical work [8], have shown that a direct correlation between contrast and structure does not necessarily represent the true situation [9] if dynamical effects have to be considered. This is the case if the sample thickness is more than $\xi_g/2$, where ξ_g is the extinction distance. It is necessary to make certain assumptions in calculating ξ_g because this sample does not possess three-dimensional crystalline order

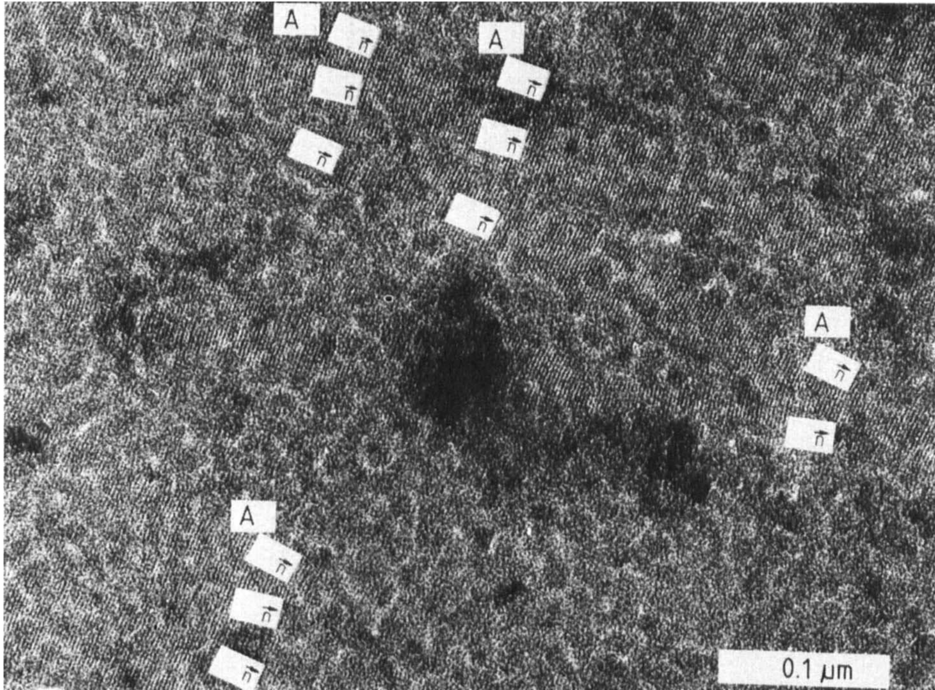

Figure 4. Bright field phase contrast image of smectic layers in the side chain liquid crystal polymer. Here **n** indicates the director orientation.

Downloaded At: 16:29 26 January 2011

but only liquid-crystalline order; i.e. the side chains are free to perform liquid-like motions whch are frozen in on cooling below the glass transition. The diffraction pattern (cf. figure 3) showing the smectic layers indicates that the smectic planes are well ordered and parallel to the electron beam while the side chains containing the mesogenic groups are, on average, perpendicular to the smectic planes (the oriented halo is perpendicular to the sharp, small angle smectic reflections). In order to estimate the extinction distance, it is necessary to use the information obtained from the single crystal microdiffraction pattern determined from the occasional regions in which the chains were oriented perpendicular to the thin films (cf. I). In that case the c direction was defined as the direction of the side chains (cf. figure 13 (b) of I). The smectic layers are then (001) planes; therefore we require the extinction distance

$$\xi_{001} = \frac{\pi V_c \cos\theta}{\lambda F_{001}},$$

where V_c is the volume of the unit cell, F_{001} is the structure factor and λ is the wavelength. The structure factor is calculated from the relationship

$$F_{hkl} = \sum_i f_i(\alpha)\exp(-2\pi i(hu_i + kv_i + lw_i)),$$

where the f_i are the scattering amplitudes for each atom and u_i, v_i, w_i are their fractional coordinates. In view of the complexity of the molecule, in which each side chain contains a large number of atoms, only the scattering of the carbon and oxygen atoms was considered, although hydrogen atoms give rise to scattering contributions which are not entirely negligible in electron diffraction. The scattering amplitudes

were taken from the *International Tables of Crystallography*, Vol. III, and the structure factors were calculated using a Fortran program originally written by D. K. Smith (UCRL 7196) and adapted by M. Stamm. From these calculations, the value of ξ for the smectic planes of interest is 1800 Å. In order to justify the kinematic approximation in interpreting the image contrast, the specimen should be less than $\xi/2 = 900$ Å thick. It was shown in the replicas of figure 6 of I that these samples consist of two or three layers, each between 50–90 Å, so that the kinematic approximation is justified.

3.7. *Image processing*

In order to stabilize the sample it was necessary to support it on a carbon film. While offering the advantage of supplying a useful test for astigmatism, the carbon film brings with it the disadvantage of introducing background noise. In order to eliminate this, there are two possible paths: (*a*) image reconstruction in a light diffractometer or (*b*) image reconstruction using a computer. Both techniques were applied to these micrographs. Unfortunately the size of the phase contrast structures in the carbon film under the defocus conditions giving optimum phase contrast transfer for the smectic planes are of comparable size to the smectic layers so that the halo produced from the carbon film in the light diffractometer are superimposed on the spots produced by the smectic layers (cf. figure 7). Consequently the spatial frequencies in the direction of the spots cannot be eliminated by filtering in the diffraction plane. Filtering of the remaining spatial frequencies did not produce entirely satisfactory results. Those from the computer processed image were more satisfactory. In this case the reconstructed image was processed by registering the grey levels in the image and eliminating image details below a certain grey level.

Downloaded At: 16:29 26 January 2011

4. Discussion of the results

For low molar mass liquid crystals, structural information is very abundant and on the basis of X-ray experiments, combined with optical microscopy and miscibility methods, it has been possible to identify twelve different smectic phases [10]. While all of these have the uniting feature of forming layered structures they are distinguished from one another by their molecular packing, molecular tilt relative to the smectic planes, in-plane correlations and layer correlations. The amount of structural information about polymer liquid crystals and, in particular, liquid crystal side chain polymers is much less abundant [11–14]. Generally the information is limited to a determination of the layer spacing and the average molecular tilt with respect to the smectic planes. There are fundamental reasons for this; for example, because of the limited order the data cannot be interpreted in a unique way. The same problem applies to the electron diffraction pattern shown in figure 3. The three orders of diffraction in the small angle spacing indicate that the smectic planes have long range order. Furthermore, the oriented amorphous halos perpendicular to them show that the side chains have an orientational order but a lack of positional order in a direction which is on average perpendicular to the smectic planes. This indicates a smectic A phase and is not new information. Careful study of the small angle maxima shows that they are extremely sharp but that they indicate some arcing ($\theta \sim 10°$). From a diffraction pattern it is impossible to decide whether this results from slight misalignment of individual blocks of straight smectic planes or whether there is misalignment within one block. Furthermore, it would be impossible to decide whether there is a

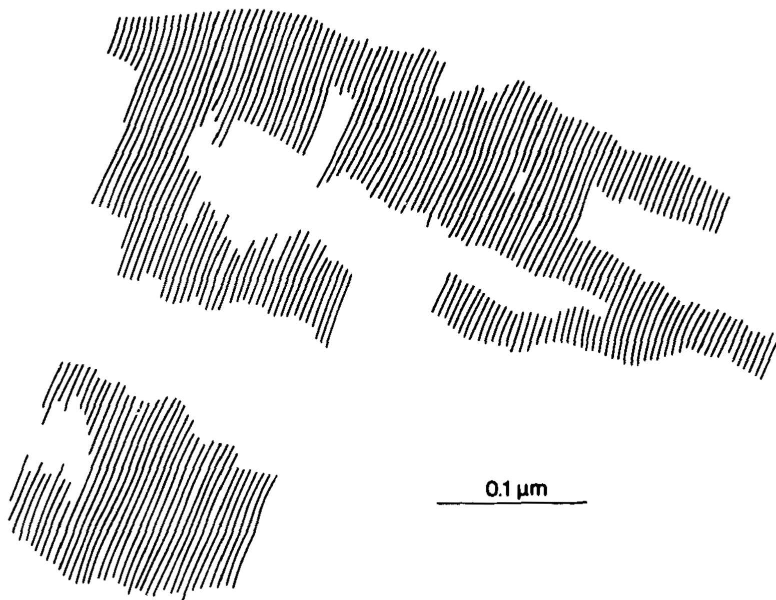

Figure 5. Transparent overlay from high magnification image of the smectic planes (every second plane is indicated).

Downloaded At: 16:29 26 January 2011

continuous range of slight orientation mismatch or whether the smectic planes are curved. By applying very stringent conditions to the imaging process it has been possible to answer this question unambiguously (cf. figure 4). The smectic planes in this particular side chain liquid-crystalline polymer are indoubtedly curved. A careful study of a region such as region A in the transparent overlay (cf. figure 5) of a high magnification micrograph is even indicative of an undulation with a wavelength of about 0·45 μm; the curvature is very slight with a radius of 1·12 μm.

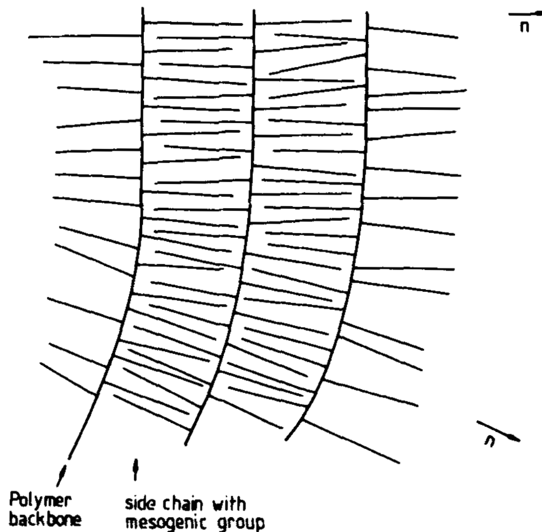

Figure 6. Chain conformation of side chain liquid crystal polymer with a polymethacrylate backbone and a biphenylester as the mesogen.

The electron micrograph has provided therefore the model which is required to interpret the diffraction pattern. It was demonstrated that the kinematic theory of image formation applies, so that modifications need not be applied to the model. For this polymer the smectic planes have a high degree of order and only very occasionally, in regions such as B, is there any indication of layer mismatch indicative of a dislocation. The range of ordering in the direction perpendicular to the smectic planes is much greater than the length of the smectic planes, a conclusion which was already inferred from the dark field micrographs of figure 9, in I; here the same argument is applied as in I. It is impossible to give information about the orientation of the liquid crystals between the regions showing contrast. The smectic planes could be tilted away from the diffraction position and, in imaging, the projection of potential in the smectic planes may be tilted away from the beam direction. It is not entirely surprising to find such a high degree of ordering in the smectic planes of this particular side chain polymer system. It was already noted in I from a study of the atomic model that the end groups fit well into the spaces provided by the spacer so that the mesogenic groups can stack rather well above one another with the side chains interlocking.

Downloaded At: 16:29 26 January 2011

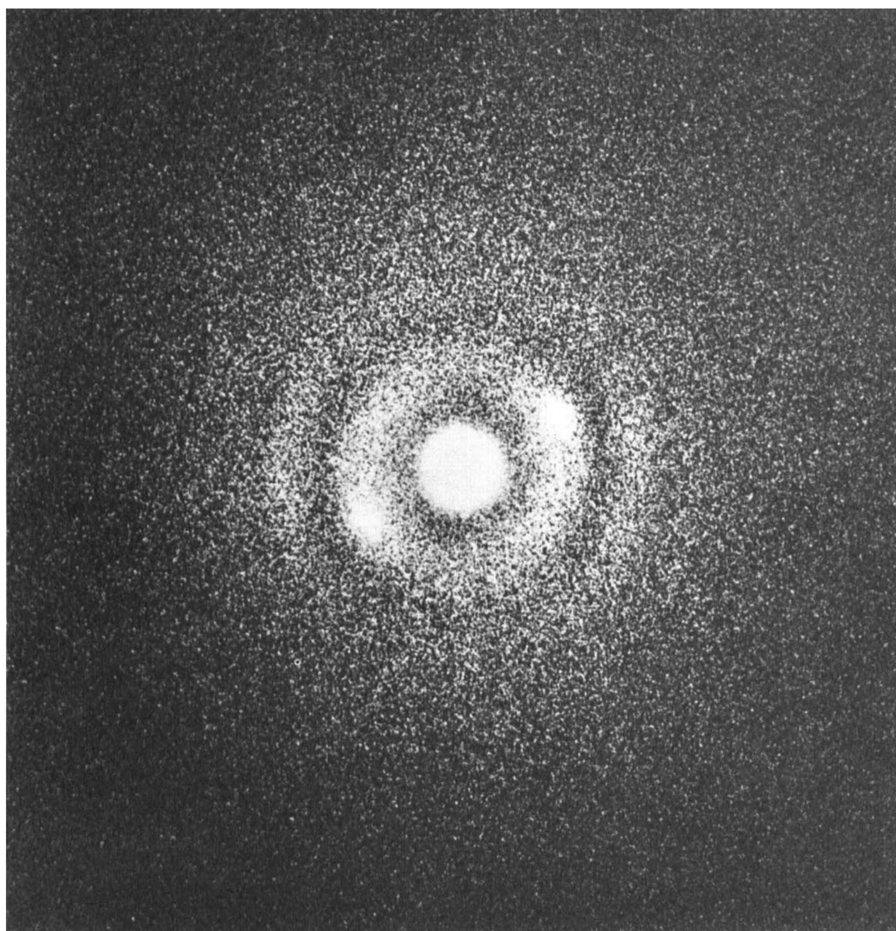

Figure 7. Optical transform of a micrograph containing lattice planes plus the carbon film.

The degree of order observed in the smectic planes differs from one polymer to another (figure 6) [15]. In view of the fact that structural details of this category can be obtained only by electron microscopy, it is clearly important as well as desirable to improve the signal-to-noise ratio in such micrographs. This turns out to be a problem, as is demonstrated in the optical transform of the micrograph showing the lattice planes. The phase contrast noise from the carbon is of the same order of magnitude as the spacing in which we are interested (cf. figure 7). In theory, the optimum defocusing can be specified as that which puts the first zero of the transfer function (the minimum after the first Thon ring) at a value of α/λ somewhat greater than the highest spatial frequency of interest. Unfortunately, for the spatial frequencies in question (corresponding to a lattice spacing of 28 Å), the optimum defocusing is already a poor compromise between low phase contrast and high frequency noise, so that optical filtering in the focal plane of the light diffractometer objective is not the best method, but should bring some improvement. Work is in progress in order to improve the quality of the computer generated images and will be discussed in connection with a paper reporting on images obtained from smectic planes, and comparing different liquid crystal polymers [15].

We are grateful to a number of colleagues for their friendly willingness to discuss various aspects of this work. These include Professor E. W. Fischer, Dr. G. Schmidt, Dr. K. Isoda, Dr. J. Petermann and Dr. J. Wendorff. We are also indepted to the Deutsche Forschungsgemeinschaft for financial support.

Downloaded At: 16:29 26 January 2011

References

[1] Crew, A. V., Isaacson, M. S., and Zeitler, E., 1979, *Advances in Structure Research*, Vol. 7, edited by W. Hoppe and R. Mason (Vieweg).
[2] Andrews, E. H., and Voigt-Martin, I. G., 1971, *Proc. R. Soc.* A, **327**, 251.
[3] Booy, F. P., and Van Bruggen, E. F. J., 1984, *Ultramicroscopy*, **3**, 337.
[4] Hoppe, W., 1971, *Phil. Trans. R. Soc.* B, **261**, 71.
[5] Thon, F., 1966, *Z. Naturf. (a)*, **21**, 476.
[6] Voigt-Martin, I. G., and Wendorff, J. H., 1985, *Encyclopedia of Polymer Science and Engineering* (Wiley), pp. 789–842.
[7] Erickson, H. P., and Klug, A., 1971, *Phil. Trans. R. Soc.* B, **261**, 105.
[8] Menter, J. W., 1956, *Proc. R. Soc.* A, **236**, 119.
[9] Cowley, J. M., 1975, *Diffraction Physics*, (North Holland).
[10] Gray, G. W., and Goodby, J. W., 1984, *Smectic Liquid Crystals* (Leonard Hill).
[11] Zugenmaier, P., and Mügge, J., 1984, *Macromolek. Chem. Suppl.*, **8**, 267.
[12] Wendorff, J. H., 1984, *Macromolek. Chem. Suppl.*, **6**, 41.
[13] Zentel, R., and Strobl, G., 1984, *Macromolek. Chem.*, **185**, 2669.
[14] Shibaev, V., 1984, *Polym. Sci. U.S.S.R.*, **26**, 370.
[15] Voigt-Martin, I. G., and Durst, H. (in preparation).